Supplementary Data
Table of Contents

Section 1. Experimental section

Table S1. List of the sequences used in this study and their structure in K^+ solutions. The structure published and the loops arrangement (from 5' to 3') are also referred *Lat*, *Diag* and *Prop* stand respectively for *Lateral*, *Diagonal* and *Propeller* loop type.

	Name	Sequence	Structure	Loops type
hTel	22GT	$(GGGTTA)_3GGGT$	Antiparallel 2-quartet[5]	Lat-Diag-Lat
	23TAG	$TA(GGGTTA)_3GGG$	Hybrid[6]	Prop-Lat-Lat
	25TAG	$TA(GGGTTA)_3GGGTT$	Hybrid[6]	Prop-Lat-Lat
	24TTG	$TT(GGGTTA)_3GGGA$	Hybrid[7]	Prop-Lat-Lat
	26TTA	$TTA(GGGTTA)_3GGGTT$	Hybrid[8]	Lat-Lat-Prop
	23AG	$A(GGGTTA)_3GGGT$	Antiparallel 2-quartet[9]	Lat-Diag-Lat
	22AG	$A(GGGTTA)_3GGG$	Hybrid / Mixture	Mixture
	22CTA	$A(GGGCTA)_3GGG$	Antiparallel 2-quartet[10]	Lat-Lat-Lat
c-myc	CMT	TTG GGA GGG TAG GGA GGG T	Parallel[11]	Prop-Prop-Prop
	CMA	TAG GGA GGG TAG GGA GGG T	Parallel[11]	Prop-Prop-Prop
	Pu24	TGA GGG TGG GGA GGG TGG GGA AGG	Parallel[12]	Prop-Prop-Prop
Other G4's	ckit1	AGG GAG GGC GCT GGG AGG AGG G	Parallel[13]	Prop-Prop-Prop
	26CEB	AAG GGT GGG TGT AAG TGT GGG TGG GT	Parallel - 1 long loop[14]	Prop-Prop-Prop
	$[TG_4T]_4$	TGGGGT	Tetramolecular parallel[15]	No loop
	$[G_4T_4G_4]_2$	GGGG TTTT GGGG	Bimolecular antiparallel[16,17]	Diag/Diag
	$[G_4T_3G_4]_2$	GGGG TTT GGGG	Bimolecular antiparallel[17]	Lat/Lat
	$G_4(T_4G_4)_3$	$GGGG\ (TTTT\ GGGG)_3$	Antiparallel 4-quartet[17]	Lat-Diag-Lat
	HIV-PRO1	TGG CCT GGG CGG GAC TGG G	Antiparallel 2-quartet[18]	Lat-Lat-Lat
	TBA	GGT TGG TGT GGT TGG	Antiparallel 2-quartet[19]	Lat-Lat-Lat
non G4	ds26	CAA TCG GAT CGA ATT CGA TCC GAT TG	Hairpin	-
	24nonG4	TGG GAT GCG ACA GAG AGG ACG GGA	Single stranded[20]	-

Oligodeoxynucleotides were purchased from Eurogentec (Seraing, Belgium) in RP-cartridge purified and lyophilized form. After solubilisation, the concentration was measured from the absorbance at 260 nm using the molar extinction coefficients from the IDT website using the Cavaluzzi-Borer correction.[21] The buffer used to fix the ionic strength was trimethylammonium acetate (TMAA, Ultra for UPLC, Fluka). TMAA and potassium chloride (KCl, >99.999%, Sigma) were purchased from Sigma-Aldrich (Sant-Quentin Fallavier, France). Ammonium acetate (BioUltra for Molecular Biology, Fluka) was also used for comparison. Injected solutions contained 10 µM DNA with either 100 mM TMAA + 1 mM KCl, or 100 mM NH_4OAc.

A LCT Premier (Waters, Manchester, UK) was used in negative ion mode. The ESI source voltage was set to 2200 V and the cone voltage to 200 V. Because ammonium is easily released from the complexes a lower voltage for the sample cone (70 V) was used for the experiments in ammonium

acetate. This value was adequate to keep intact the fragile dimeric $[G_4T_4G_4]_2$ G-quadruplex. The source temperature was 60 °C and the pressure was increased to 45 mbar and measured using a Center Two probe (Oerlikon Leybold Vacuum, Cologne, Germany). The flow rate for the syringe pump was 200 µL/h. Shown MS spectra are the sum of ~200 scans, smoothed and baseline-subtracted using the MassLynx software.

MS/MS experiments were performed on a Bruker Amazon SL (Bremen, Germany). The ions were trapped with a trap drive voltage of 92 V, maximizing the signal of the 6- charge state. We isolated the G-quadruplex before activation for 70 ms with 1.1 V for the free G-quadruplex and 1.3V for the G-quadruplex with one and two ligands.

The CD samples were prepared as for the MS experiments. Experiments were run at 20 °C for 3 accumulations. CD spectra were normalized to molar circular dichroic absorption (Δε) based on the G-quadruplex concentration following equation 3:

$$\Delta\varepsilon=\theta/(32980\times C\times l)$$

Where θ is the ellipticity in millidegrees, C is the G-quadruplex concentration (10 µM) and l is the optical path length of the cell (0.2 cm).

Section 2. Metal complexes synthesis

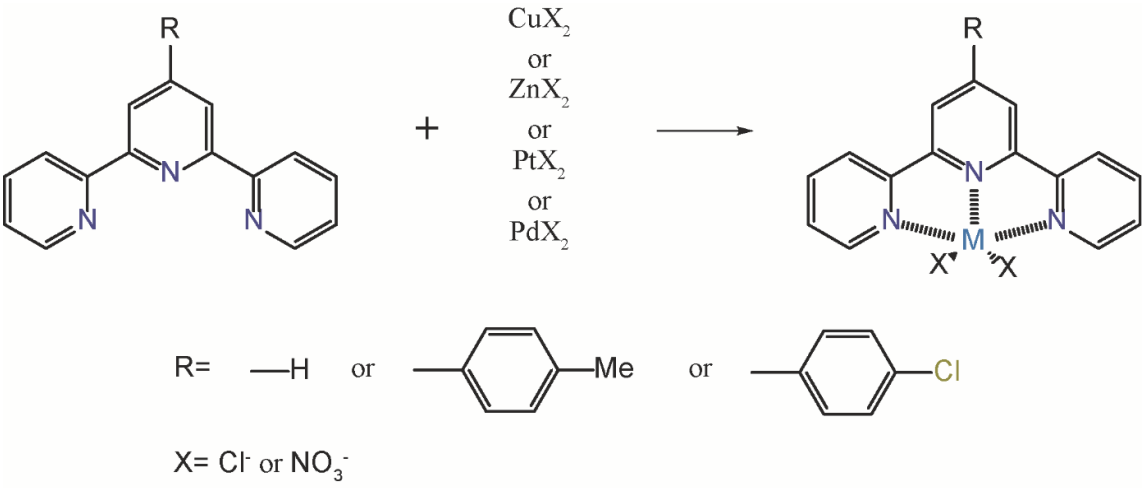

Scheme 1. Representation of the synthesis of the complexes.

For Cu-complexes:[22] The terpyridine derivative was solubilized in a vial in a minimum of dry dichloromethane. The metal salts previously solubilized in acetonitrile were added gently dropwise on the ligand solution to form two phases. The vial was put at 4 °C in the dark for one day. Crystals are formed at the interphase corresponding to the desired product. The purifications were performed washing three times with anhydrous acetonitrile, three times with dichloromethane and three times with diethyl ether. The salts were then dried under vacuum. Chemical yields were between 35 and 50%.

For Zn-complexes:[23] The same procedure as for the Cu-complexes was used except that the reaction was performed stirring under Ar for 24 hours and purified using diethyl ether. It was then dried under vacuum overnight.

For Pt-complexes:[23] The suspension of $Pt(COD)Cl_2$ in MeOH was heated at 50 °C under Ar. One equivalent of the terpyridine compound in dichloromethane was added and the mixture was stirred under Ar for 3 hours, protected from light. The solid was centrifuged and washed using EtOH and diethyl ether. It was then dried under vacuum overnight.

For Pd-complexes:[22] The same procedure as for the Cu-complexes was used except that the reaction was performed stirring under Ar for 48 hours, protected from light, and purified using dimethylformamide, dichloromethane and diethyl ether. It was then dried under vacuum for two days.

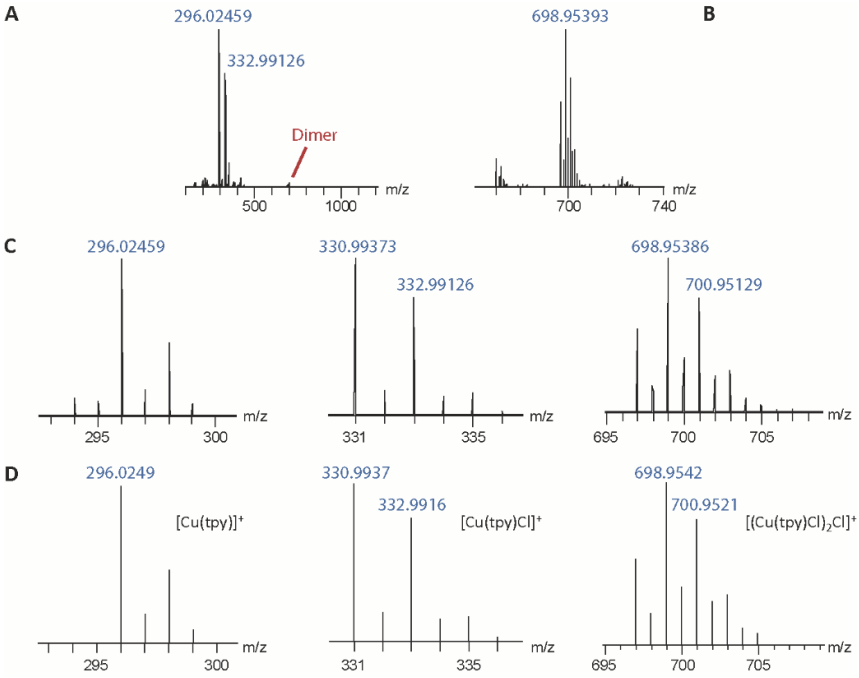

Figure S1. HRMS of Cu-tpy Cl^- salt. A) full range spectrum, B) zoom in the dimer, C) selected experimental spectra and D) theoretical spectra for the indicated formula.

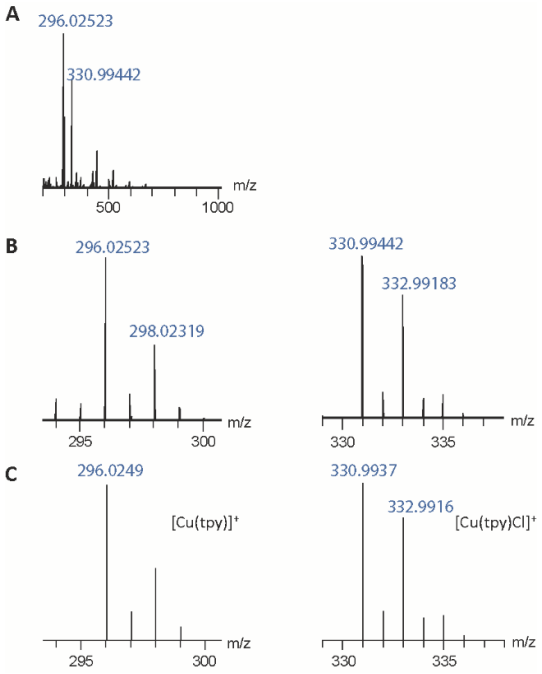

Figure S2. HRMS of Cu-tpy NO_3^- salt. A) full range spectrum, B) selected experimental spectra and C) theoretical spectra for the indicated formula.

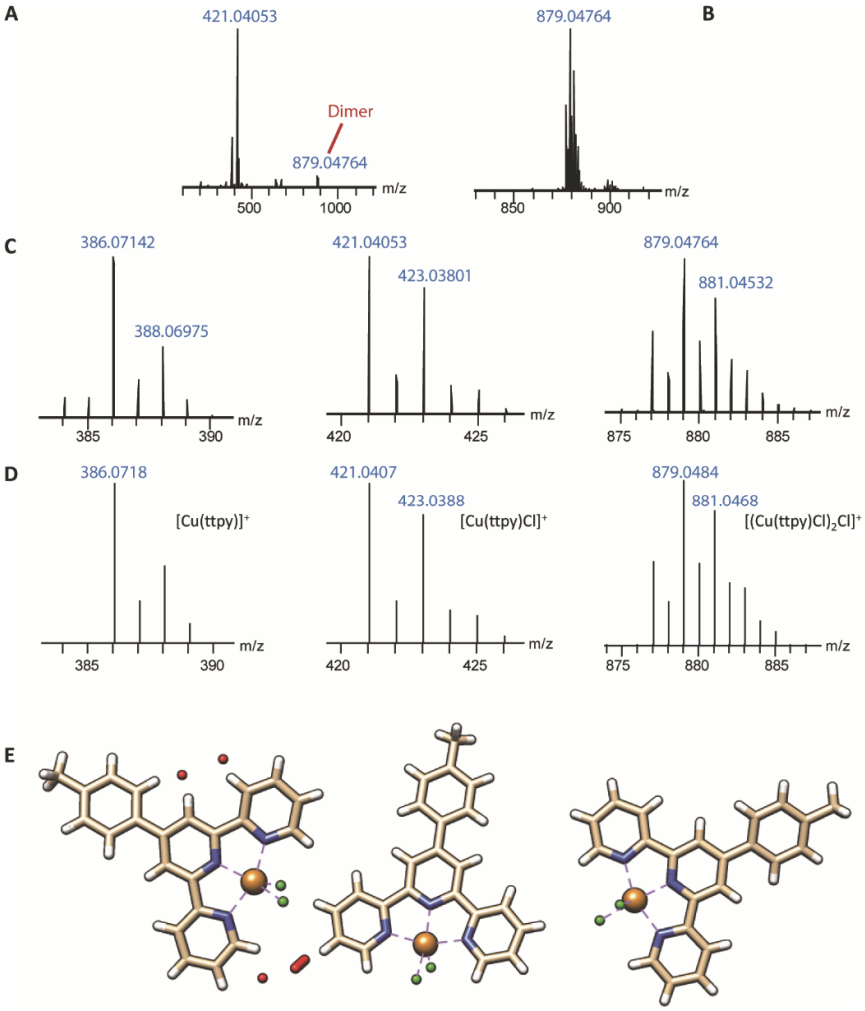

Figure S3. Characterization of Cu-ttpy Cl^- salt. A) full range HRMS spectrum, B) zoom in the dimer, C) selected experimental spectra and D) theoretical spectra for the indicated formula. E) X-ray crystal structure of the metal complex. The Cu^{2+} core is pentacoordinated: 3 coordinations come from the ttpy and 2 from two Cl^- anions.

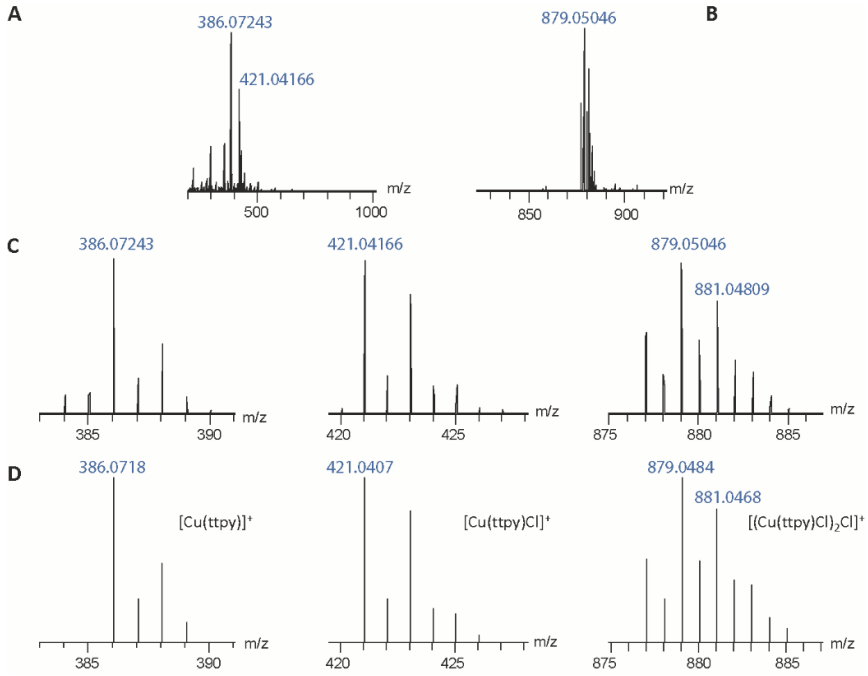

Figure S4. HRMS of Cu-ttpy NO_3^- salt. A) full range spectrum, B) zoom in the dimer, C) selected experimental spectra and D) theoretical spectra for the indicated formula.

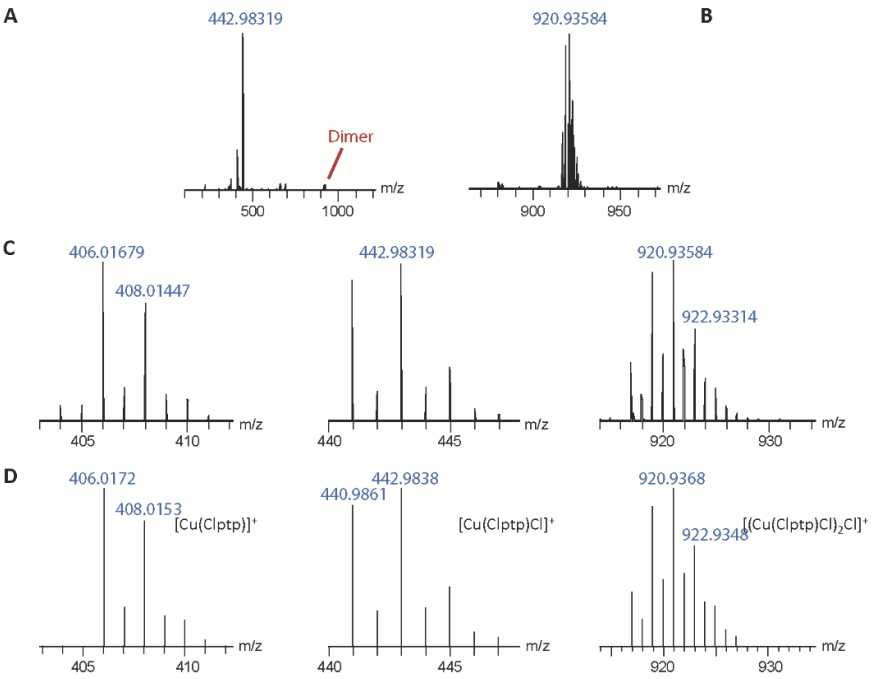

Figure S5. HRMS of Cu-Clptp Cl^- salt. A) full range spectrum, B) zoom in the dimer, C) selected experimental spectra and D) theoretical spectra for the indicated formula.

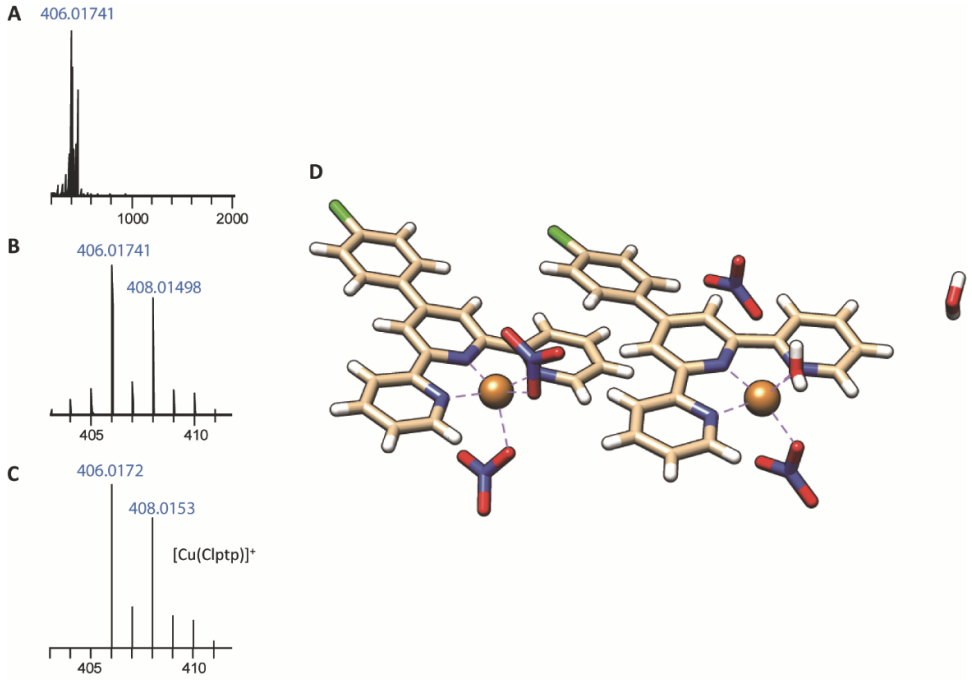

Figure S6. Characterization of Cu-Clptp NO_3^- salt. A) full range HRMS spectrum, B) selected experimental spectra and C) theoretical spectra for the indicated formula. D) X-ray crystal structure of the metal complex. The Cu^{2+} core is pentacoordinated: 3 coordinations come from the Clptp and 2 from two NO_3^- anions. One of the NO_3^- can also be replaced by a H_2O molecule.

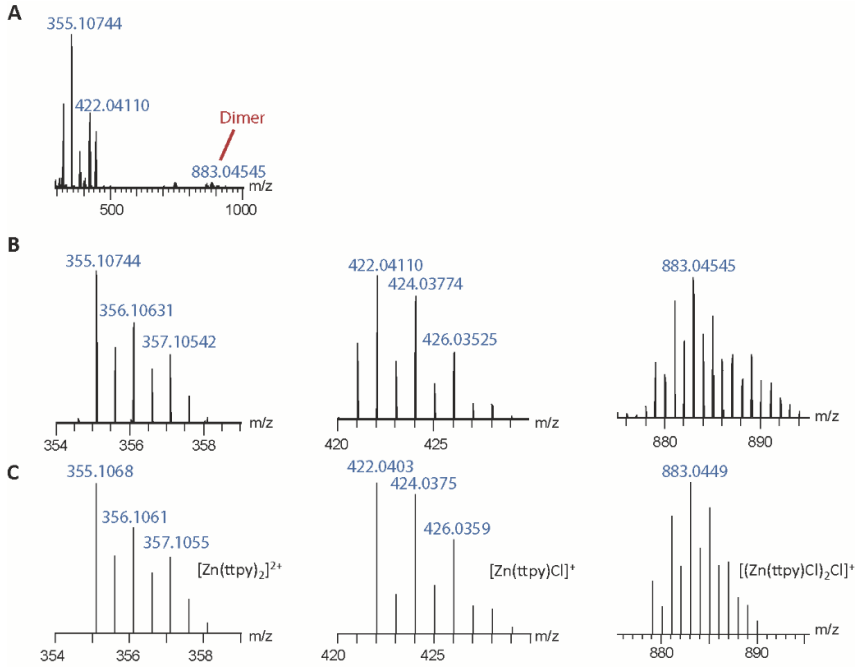

Figure S7. HRMS of Zn-ttpy Cl^- salt. A) full range spectrum, B) selected experimental spectra and C) theoretical spectra for the indicated formula.

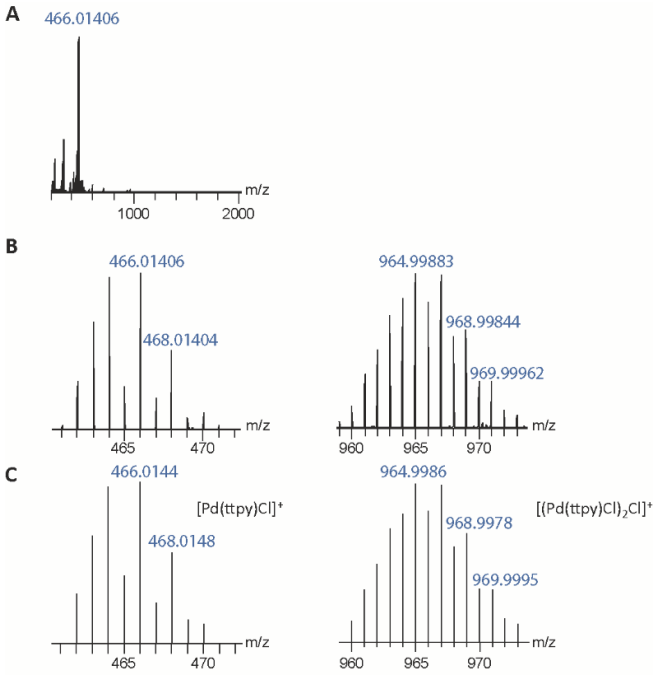

Figure S8. HRMS of Pd-ttpy Cl^- salt. A) full range spectrum, B) selected experimental spectra and C) theoretical spectra for the indicated formula.

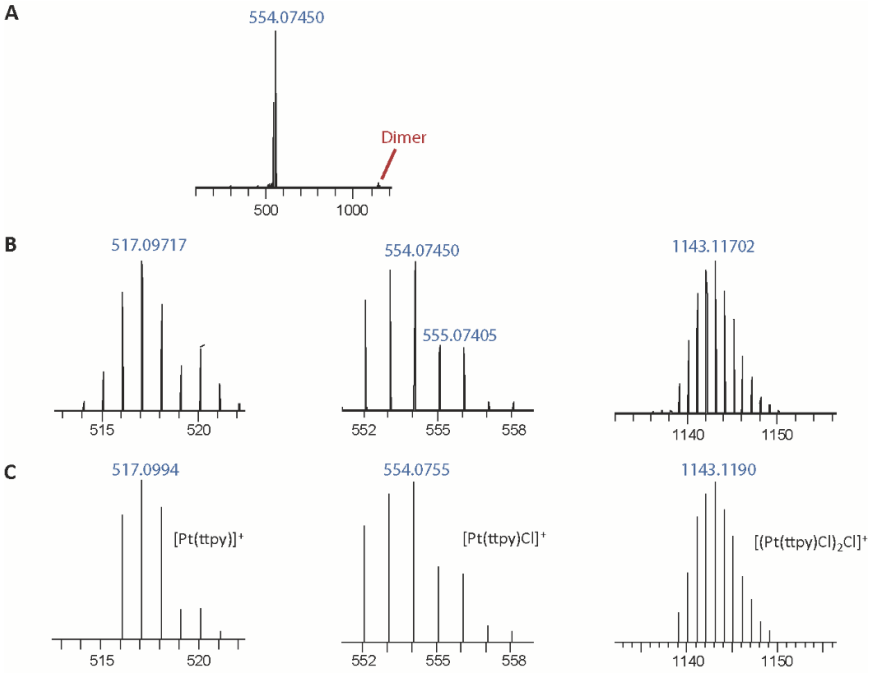

Figure S9. HRMS of Pt-ttpy Cl^- salt. A) full range spectrum, B) selected experimental spectra and C) theoretical spectra for the indicated formula.

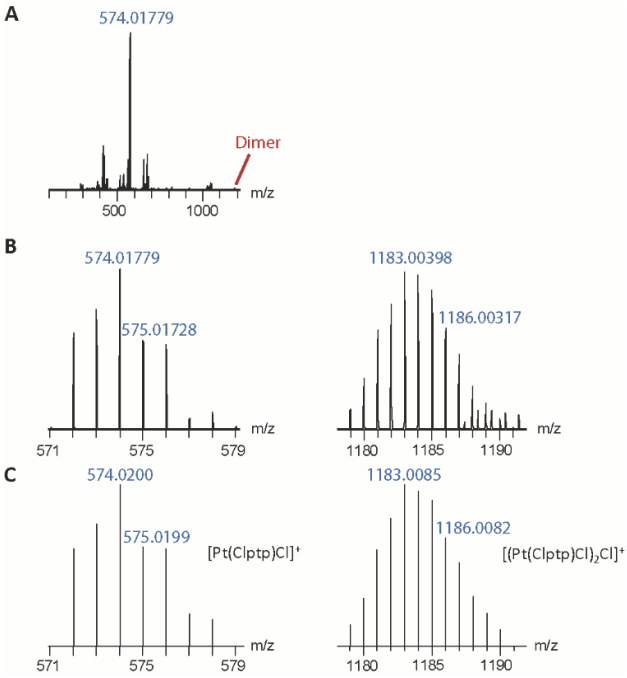

Figure S10. HRMS of Pt-Clptp Cl^- salt. A) full range spectrum, B) selected experimental spectra and C) theoretical spectra for the indicated formula.

Table S2. Crystal data and structure refinement for Cu-*ttpy* and Cu-*Clptp*.

Identification code	*Cu-ttpy*		*Cu-Clptp*	
Empirical formula	C_{66} H_{57} Cl_6 Cu_3 N_9 O_3		C_{42} H_{32} Cl_2 Cu_2 N_{10} O_{14}	
Formula weight	1427.53		1098.76	
Temperature	103(2) K		103(2) K	
Wavelength	1.54187 Å		1.54187 Å	
Crystal system	Monoclinic		Monoclinic	
Space group	P21/n		P21/c	
Unit cell dimensions	a = 10.824(6) Å	a= 90°.	a = 14.497(5) Å	a= 90°.
	b = 23.346(13) Å	b= 101.313(11)°.	b = 14.961(5) Å	b= 104.458(12)°.
	c = 24.349(12) Å	g = 90°.	c = 20.208(7) Å	g = 90°.
Volume	6033(6) $Å^3$		4244(3) $Å^3$	
Z	4		4	
Density (calculated)	1.572 Mg/m^3		1.720 Mg/m^3	
Absorption coefficient	4.130 mm^{-1}		3.129 mm^{-1}	
F(000)	2916		2232	
Crystal size	0.07 x 0.04 x 0.01 mm^3		0.03 x 0.01 x 0.01 mm^3	
Theta range for data collection	6.39 to 68.25°.		6.33 to 68.25°.	
Index ranges	-12<=h<=9, -27<=k<=28, -29<=l<=29		-17<=h<=12, -18<=k<=12, -19<=l<=24	
Reflections collected	41936		23117	
Independent reflections	10912 [R(int) = 0.1234]		7668 [R(int) = 0.0435]	
Completeness to theta = 68.25°	98.90%		98.70%	
Absorption correction	Semi-empirical from equivalents		Semi-empirical from equivalents	
Max. and min. transmission	0.9599 and 0.7609		0.9694 and 0.9120	
Refinement method	Full-matrix least-squares on F^2		Full-matrix least-squares on F^2	
Data / restraints / parameters	10912 / 0 / 796		7668 / 0 / 647	
Goodness-of-fit on F2	1.04		1.019	
Final R indices [I>2sigma(I)]	R1 = 0.0661, wR2 = 0.1551		R1 = 0.0315, wR2 = 0.0685	
R indices (all data)	R1 = 0.1165, wR2 = 0.1802		R1 = 0.0498, wR2 = 0.0720	
Largest diff. peak and hole	1.605 and -0.767 $e.Å^{-3}$		0.332 and -0.328 $e.Å^{-3}$	
Summary of Data CCDC	1475809		1475808	

Section 3. Binding affinities and cooperativity

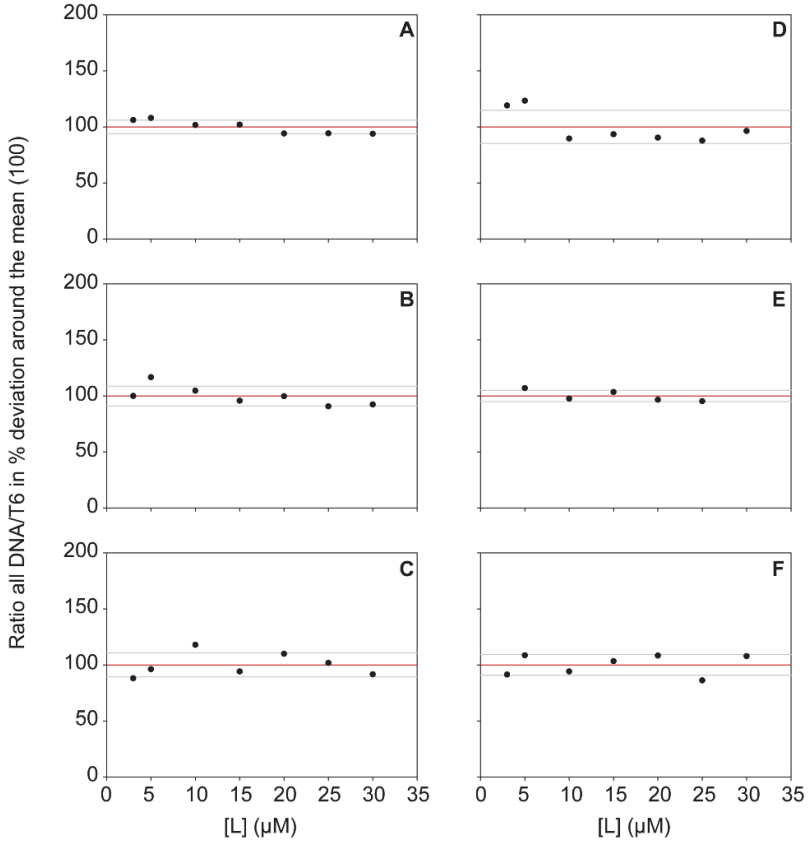

Figure S11. Evolution of the ratio between the total DNA signal of the 5- charge state and the internal standard dT6 in function of the ligand concentration in percentage of deviation around the mean for (A and D) 22GT, (B and E) Pu24 and (C and F) $[G_4T_4G_4]_2$ with (A to C) Cu-ttpy and (D to F) Cu-Clptp. In black the experimental points, in red the mean and grey the standard deviation. There is no systematic deviation from the mean value upon titration, indicating that the response factors are equal for the different complexes.

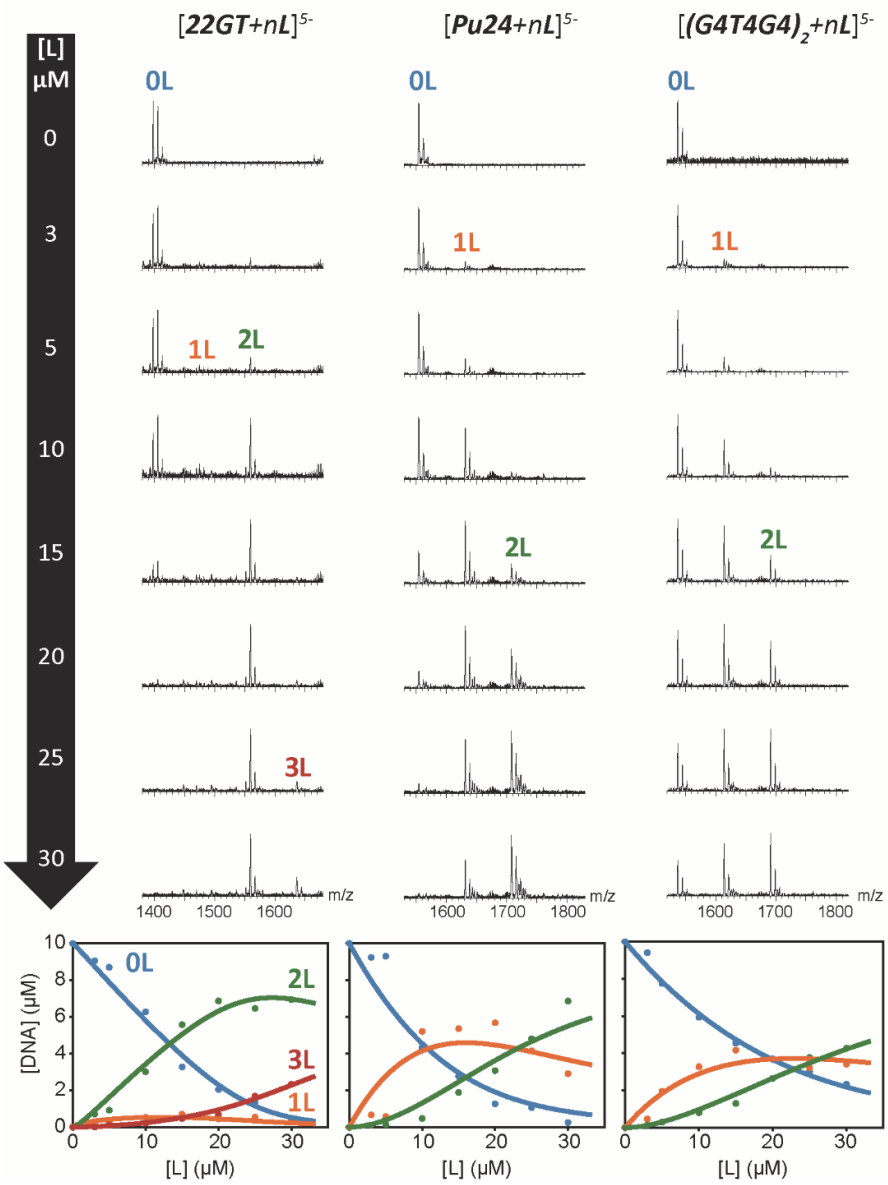

Figure S12. Top: titration of 10 µM 22GT, Pu24 or $[G4T4G4]_2$ by Cu-ttpy in 100 mM TMAA + 1 mM KCl. Zooms on the 5- charge state. Bottom: quantification and fitting.

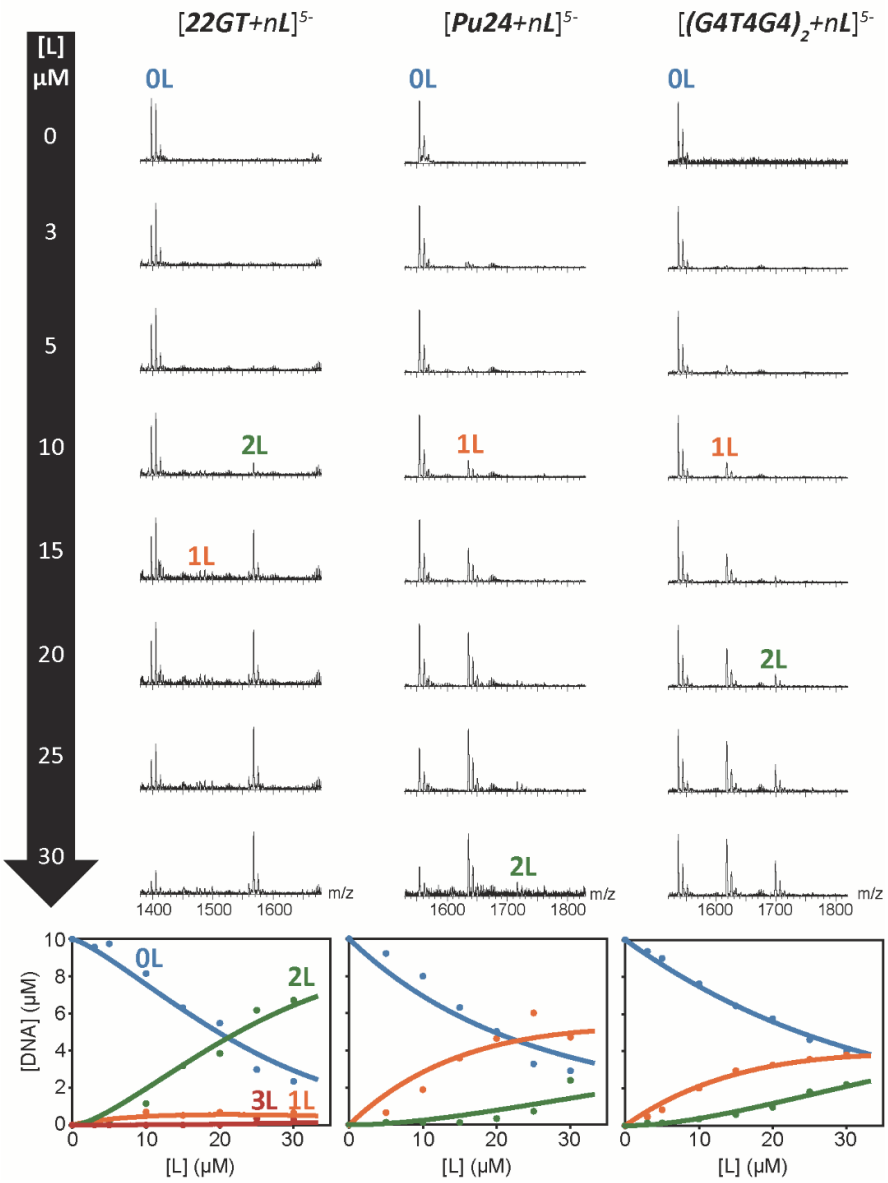

Figure S13. Top: titration of 10 µM 22GT, Pu24 or $[G4T4G4]_2$ by Cu-Clptp in 100 mM TMAA + 1 mM KCl. Zooms on the 5- charge state. Bottom: quantification and fitting.

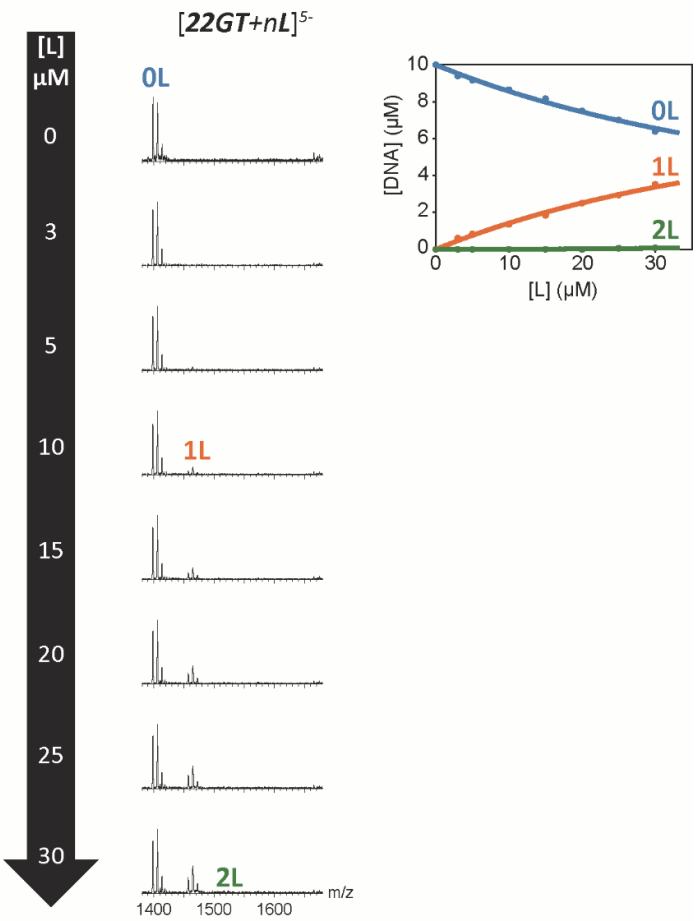

Figure S14. Left, titration of 10 µM 22GT by Cu-tpy in 100 mM TMAA + 1 mM KCl. Zooms on the 5- charge state. Right, quantification and fitting.

Table S3. K_D's obtained for the Cu-complexes (In red, the values coming from titrations, in blue from single concentration experiments). The sequences are ranked according to their K_{D1}/K_{D2} ratio for Cu-ttpy. The global K_Ds of the telomeric sequences (repeats of TTAGGG) are highlighted in blue. We calculated the equilibrium constants for each single point in the titration and calculated the standard deviation so that we can estimate the errors made on the single points K_D values: the error is less than 10%.

	Cu-ttpy				Cu-Clptp				Cu-tpy			
	log K_{D1}	log K_{D2}	log(K_{D1}*K_{D2})	K_{D1}/K_{D2}	log K_{D1}	log K_{D2}	log(K_{D1}*K_{D2})	K_{D1}/K_{D2}	log K_{D1}	log K_{D2}	log(K_{D1}*K_{D2})	K_{D1}/K_{D2}
22GT	-4.7 ± 0.4	-6.5 ± 0.2	-11.2	73	-4.0 ± 0.2	-5.9 ± 0.3	-9.9	69	-4.3 ± 0.1	-	-	-
25TAG	-5.5	-7.2	-12.7	49	-5.6	-7.1	-12.8	33	-4.6	-	-	-
23TAG	-5.7	-6.7	-12.4	9	-5.8	-6.4	-12.2	4	-4.6	-	-	-
24TTG	-5.5	-6.4	-11.9	7	-4.9	-5.6	-10.4	5	-4.3	-	-	-
26TTA	-5.1	-5.7	-10.8	5	-4.8	-5.8	-10.6	9	-5.0	-	-	-
23AG	-5.8	-5.9	-11.7	1.4	-5.4	-5.7	-11.0	2.1	-4.8	-	-	-
$[G4T3G4]_2$	-4.6	-4.6	-9.3	1.0	-4.7	-4.5	-9.2	0.6	-4.0	-	-	-
22AG	-6.1	-5.9	-12.0	0.7	-6.3	-5.9	-12.2	0.4	-4.5	-	-	-
$[G4T4G4]_2$	-5.0 ± 0.2	-4.8 ± 0.2	-9.8	0.7	-4.6 ± 0.1	-4.4 ± 0.3	-9.0	0.6	-4.2	-	-	-
24nonG4	-4.7	-4.3	-9.0	0.48	-4.6	-4.5	-9.0	0.78	-4.0	-	-	-
CMA	-5.2	-4.8	-10.0	0.37	-5.0	-4.5	-9.5	0.33	-4.8	-	-	-
Pu24	-5.5 ± 0.7	-5.0 ± 0.3	-10.4	0.35	-4.8 ± 0.3	-4.1 ± 0.5	-8.9	0.21	-4.8	-	-	-
22CTA	-5.2	-4.7	-9.9	0.34	-5.3	-4.8	-10.1	0.27	-4.7	-	-	-
CMT	-5.8	-5.3	-11.0	0.33	-5.5	-5.0	-10.5	0.36	-5.1	-4.8	-9.9	0.4
26CEB	-5.2	-4.3	-9.6	0.13	-5.1	-4.0	-9.2	0.08	-5.0	-4.1	-	0.1
$[TG4T]_4$	-5.2	-4.1	-9.4	0.08	-5.0	-4.3	-9.3	0.20	-3.7	-	-	-
$G4(T4G4)_3$	-6.0	-4.5	-10.5	0.03	-6.1	-4.6	-10.7	0.04	-5.3	-	-	-
ds26	-4.2	-	-	-	-4.0	-	-	-	-4.2	-	-	-
HIV	-	-	-	-	-	-	-	-	-4.2	-	-	-
ckit1	-	-	-	-	-	-	-	-	-	-	-	-
TBA	-	-	-	-	-	-	-	-	-	-	-	-

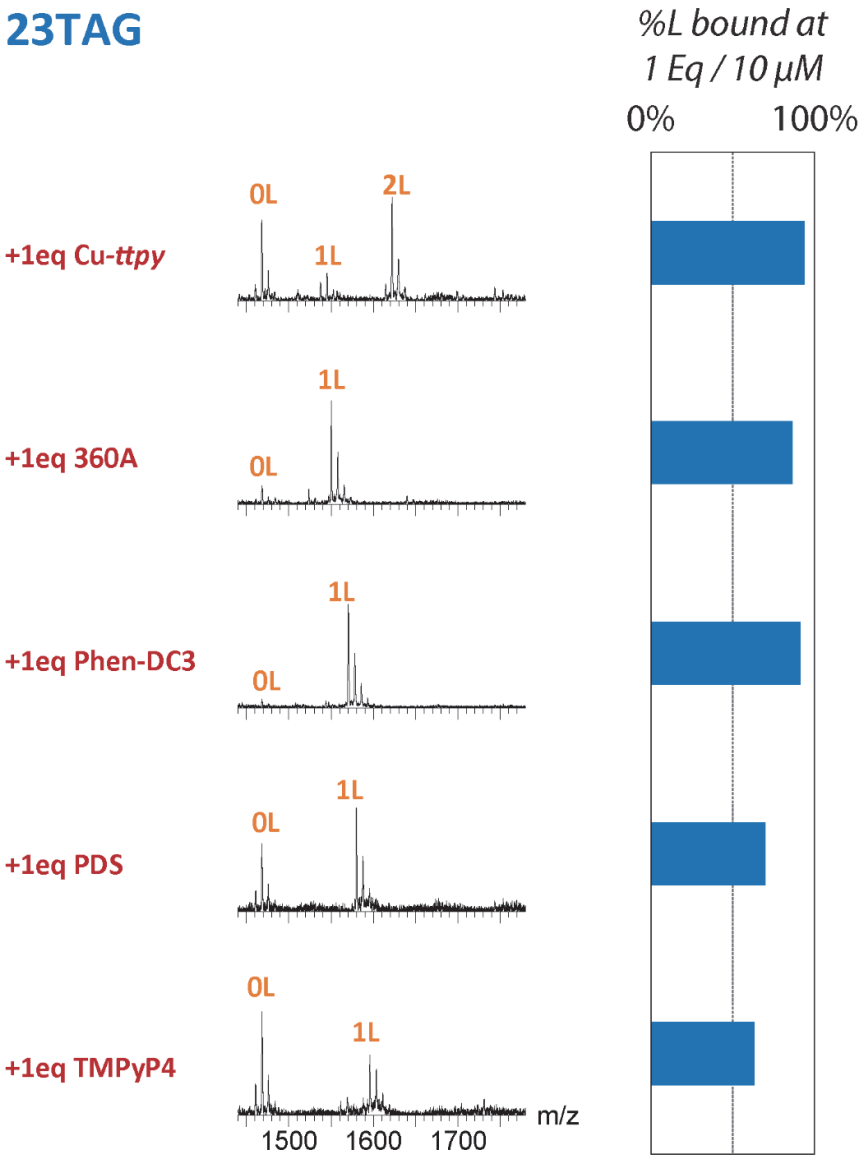

Figure S15. MS spectra of 23TAG with 1 eq Cu-ttpy, 360A,[1,2] Phen-DC3,[3] PDS (pyridostatin)[4] and TMPyP4, respectively, in 100 mM TMAA + 1 mM KCl. The amount of ligand bound was quantified: Cu-ttpy binds the hTel G4 with affinities as good as 360A and Phen-DC3.

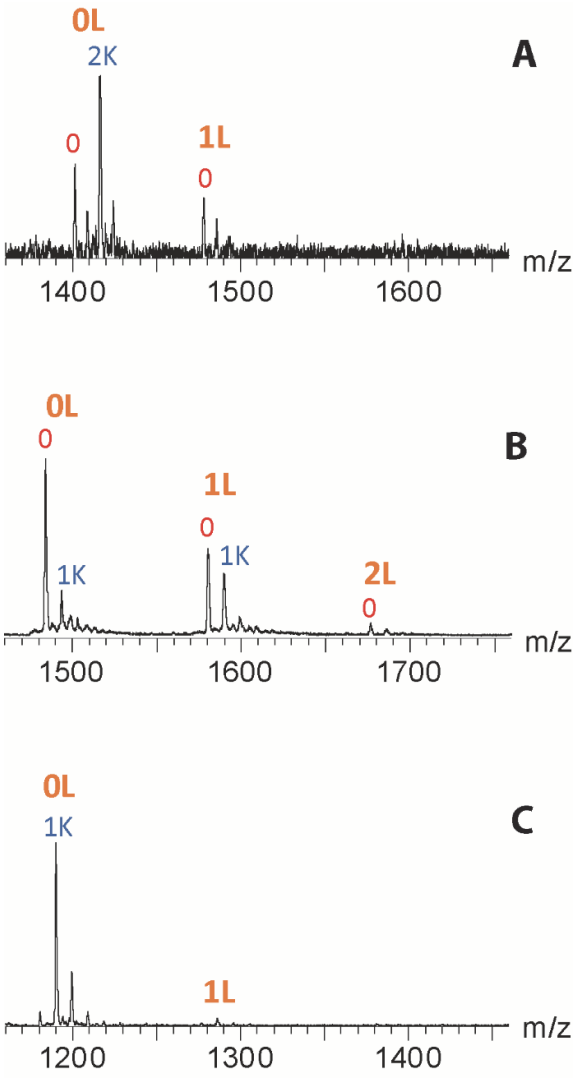

Figure S16. MS spectra of 10 µM A) ckit1, B) HIV-PRO1 and C) TBA in 100 mM TMAA + 1 mM KCl with 10 µM Cu-ttpy. The ligand does not bind to TBA and only to the species that do not contain potassium for ckit1. On the other hand the fraction of DNA with 1-K^+ is increased when bound to the ligand, which could indicate that G-quadruplex folding is induced.

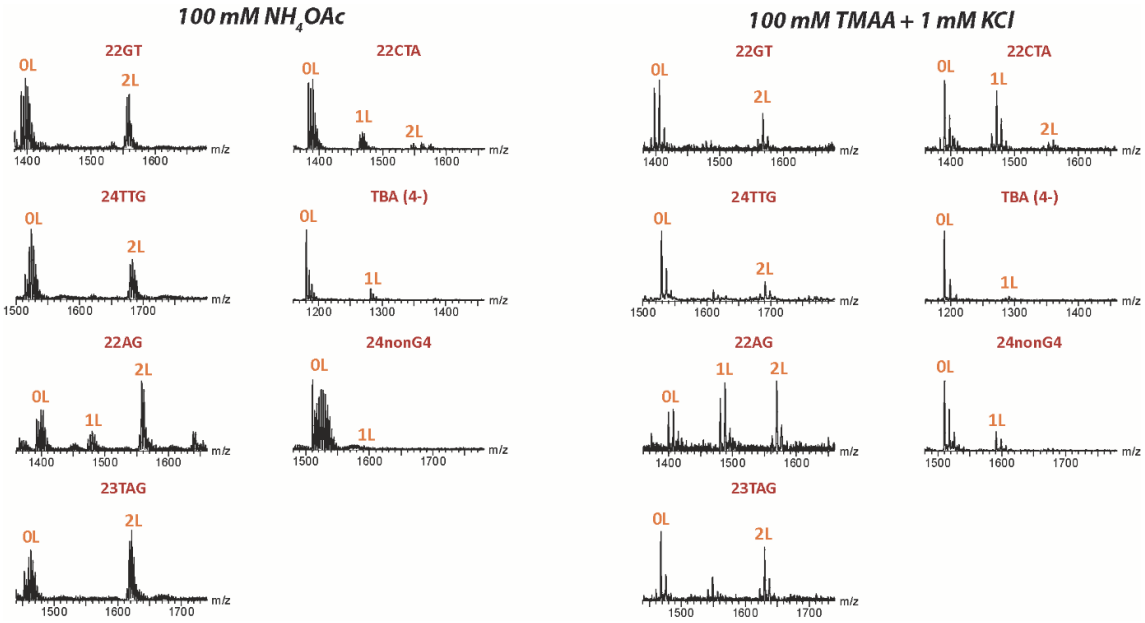

Figure S17. MS spectra of 10 µM DNA in 100 mM NH4OAc or 100 mM TMAA + 1 mM KCl with 10 µM Cu-Clptp. The results are similar in both conditions: the binding of this ligands is cooperative for the human telomeric sequences.

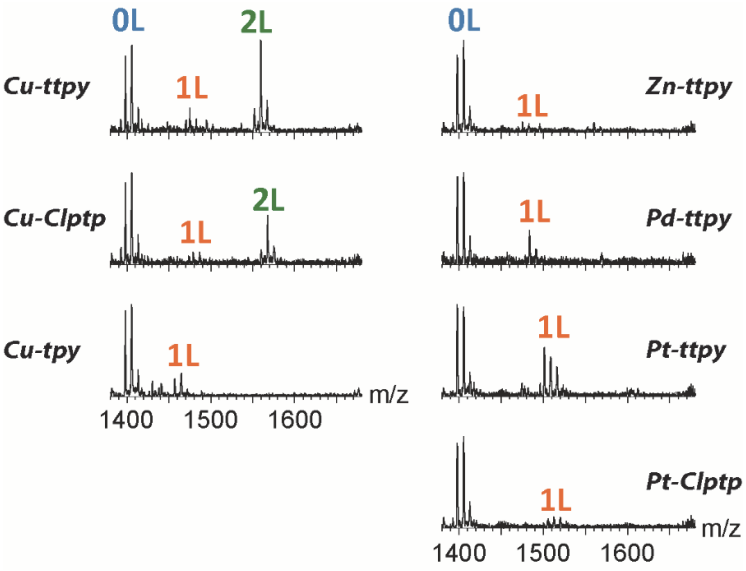

Figure S18. Comparison of the cooperativity of binding of different metal complexes on 22GT. ESI-MS of 10 µM 22GT in 100 mM TMAA + 1 mM KCl with 10 µM of ligands.

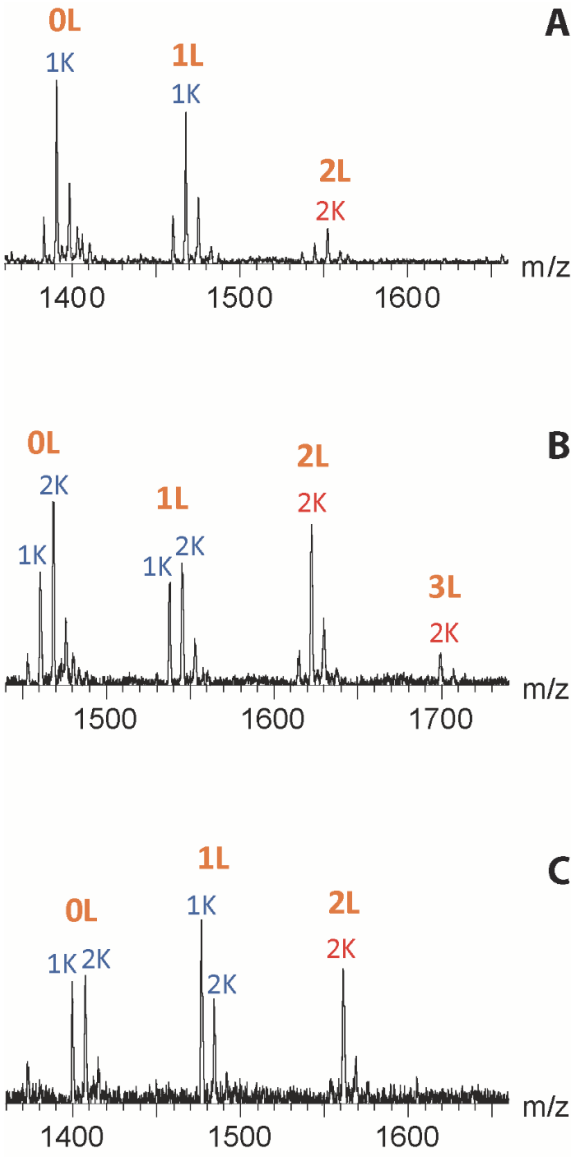

Figure S19. MS spectra of 10 µM (A) 22CTA, (B) 23AG and (C) 22AG in 100 mM TMAA + 1 mM KCl with 10 µM Cu-ttpy ligand (L)*. When two ligands are bound the main potassium stoichiometry is 2-K^+.*

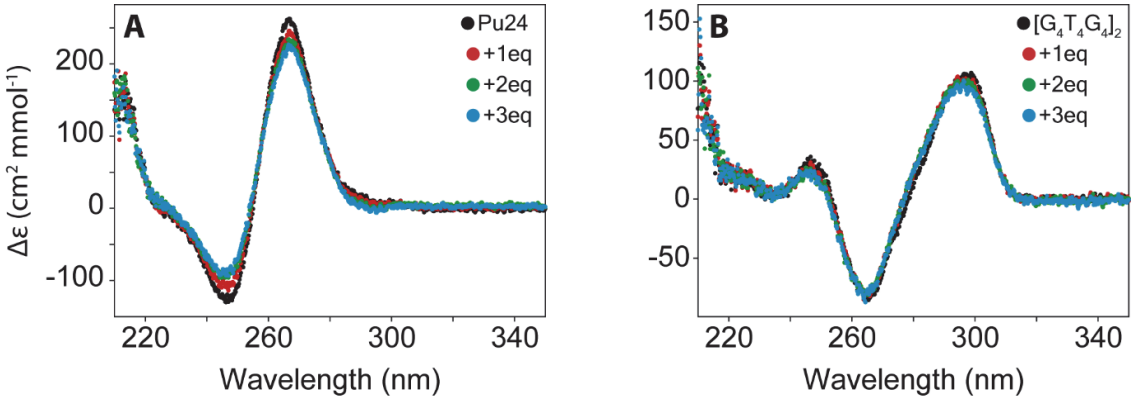

Figure S20. CD of (A) Pu24 and (B) $[G4T4G4]_2$ in presence of increasing amount of Cu-ttpy ligand.

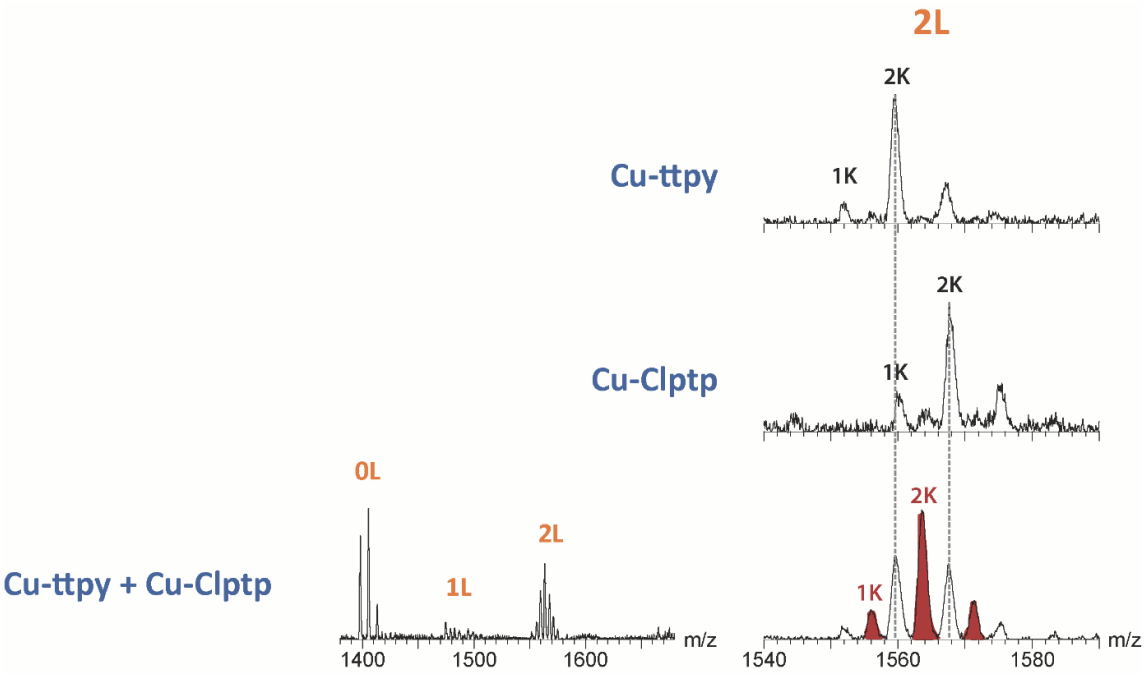

Figure S21. Competition experiment: MS spectra of 10 µM 22GT in 100 mM TMAA + 1 mM KCl with 10 µM (A) Cu-ttpy, (B) Cu-Clptp and (C) 10 µM of each ligand. When two ligands are bound the main potassium stoichiometry is 2K. There is a statistical distribution of stoichiometries: 2x Cuttpy, 2x CuClptp and 1+1. *The red-colored peaks can only be attributed to the heterodimer bound to 22GT.*

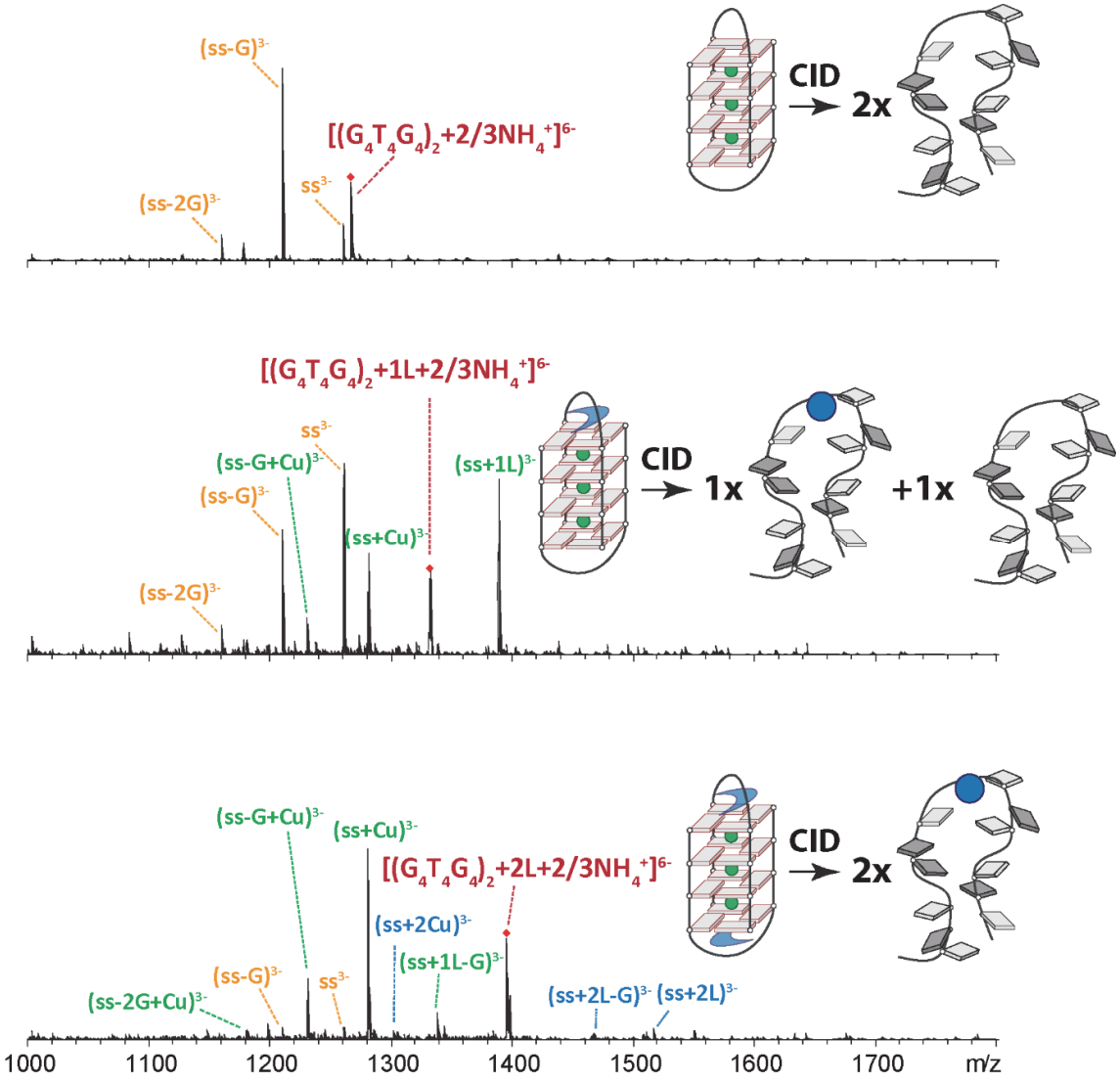

Figure S22. MS/MS spectra of 40 µM $(G_4T_4G_4)_2$ in 100 mM NH_4OAc with 60 µM (A) Cu-ttpy. Top, selection of $[(G_4T_4G_4)_2+2/3NH_4^+]^{6-}$ and activation with 1.1 V, middle, selection of $[(G_4T_4G_4)_2+\mathbf{1L}+2/3NH_4^+]^{6-}$ and activation with 1.3 V and bottom, selection of $[(G_4T_4G_4)_2+\mathbf{2L}+2/3NH_4+]^{6-}$ and activation with 1.3 V.

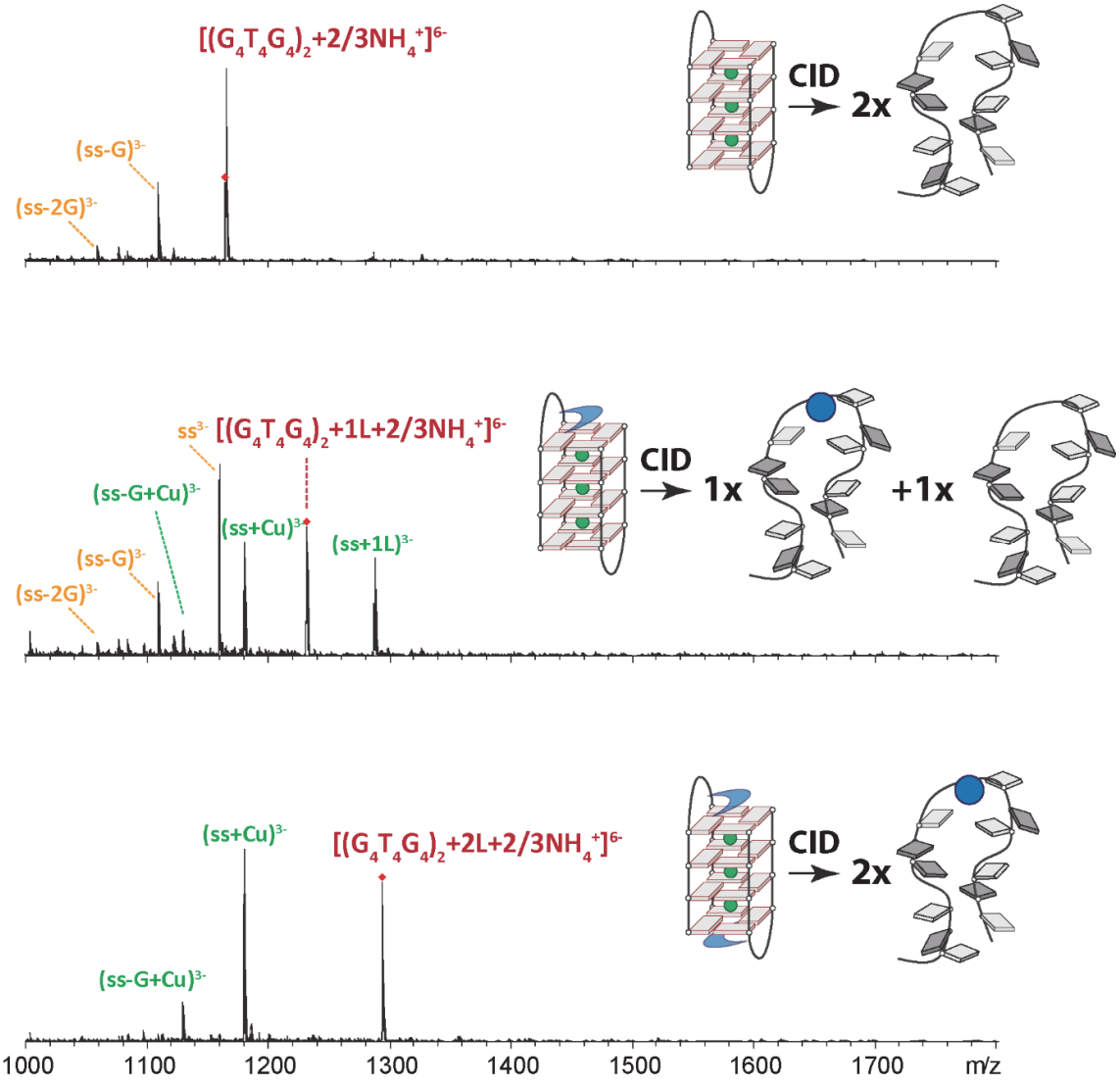

Figure S23. MS/MS spectra of 40 µM $(G_4T_3G_4)_2$ in 100 mM NH_4OAc with 60 µM (A) Cu-ttpy. Top, selection of $[(G_4T_3G_4)_2+2/3NH_4^+]^{6-}$ and activation with 1.1 V, middle, selection of $[(G_4T_3G_4)_2+\mathbf{1L}+2/3NH_4^+]^{6-}$ and activation with 1.3 V and bottom, selection of $[(G_4T_3G_4)_2+\mathbf{2L}+2/3NH_4+]^{6-}$ and activation with 1.3 V.

Section 4. Supplementary references

1 A. De Cian and J.-L. Mergny, *Nucleic Acids Res.*, 2007, **35**, 2483–93.

2 C. Granotier, G. Pennarun, L. Riou, F. Hoffschir, L. R. Gauthier, A. De Cian, D. Gomez, E. Mandine, J.-F. Riou, J.-L. Mergny, P. Mailliet, B. Dutrillaux and F. D. Boussin, *Nucleic Acids Res.*, 2005, **33**, 4182–90.

3 A. De Cian, E. Delemos, J.-L. Mergny, M.-P. Teulade-Fichou and D. Monchaud, *J. Am. Chem. Soc.*, 2007, **129**, 1856–7.

4 D. Koirala, S. Dhakal, B. Ashbridge, Y. Sannohe, R. Rodriguez, H. Sugiyama, S. Balasubramanian and H. Mao, *Nat. Chem.*, 2011, **3**, 782–7.

5 K. W. Lim, S. Amrane, S. Bouaziz, W. Xu, Y. Mu, D. J. Patel, K. N. Luu and A. T. Phan, *J. Am. Chem. Soc.*, 2009, **131**, 4301–9.

6 A. T. Phan, V. Kuryavyi, K. N. Luu and D. J. Patel, *Nucleic Acids Res.*, 2007, **35**, 6517–25.

7 K. N. Luu, A. T. Phan, V. Kuryavyi, L. Lacroix and D. J. Patel, *J. Am. Chem. Soc.*, 2006, **128**, 9963–70.

8 J. Dai, M. Carver, C. Punchihewa, R. A. Jones and D. Yang, *Nucleic Acids Res.*, 2007, **35**, 4927–4940.

9 Z. Zhang, J. Dai, E. Veliath, R. A. Jones and D. Yang, *Nucleic Acids Res.*, 2010, **38**, 1009–1021.

10 K. W. Lim, P. Alberti, A. Guédin, L. Lacroix, J. F. Riou, N. J. Royle, J. L. Mergny and A. T. Phan, *Nucleic Acids Res.*, 2009, **37**, 6239–6248.

11 M. Trajkovski, E. Morel, F. Hamon, S. Bombard, M.-P. Teulade-Fichou and J. Plavec, *Chem. - A Eur. J.*, 2015, **21**, 7798–7807.

12 A. T. Phan, V. Kuryavyi, H. Y. Gaw and D. J. Patel, *Nat. Chem. Biol.*, 2005, **1**, 167–173.

13 A. T. Phan, V. Kuryavyi, S. Burge, S. Neidle and D. J. Patel, *J. Am. Chem. Soc.*, 2007, **129**, 4386–92.

14 S. Amrane, M. Adrian, B. Heddi, A. Serero, A. Nicolas, J. Mergny and A. T. Phan, *J. Am. Chem. Soc.*, 2012, **134**, 5807–5816.

15 G. Laughlan, A. Murchie, D. Norman, M. Moore, P. Moody, D. Lilley and B. Luisi, *Science (80-.).*, 1994, **265**, 520–524.

16 P. Schultze, F. W. Smith and J. Feigon, *Structure*, 1994, **2**, 221–233.

17 F. Balthasart, J. Plavec and V. Gabelica, *J. Am. Soc. Mass Spectrom.*, 2013, **24**, 1–8.

18 S. Amrane, A. Kerkour, A. Bedrat, B. Vialet, M.-L. Andreola and J.-L. Mergny, *J. Am. Chem. Soc.*, 2014, **136**, 5249–52.

19 R. F. Macaya, P. Schultze, F. W. Smith, J. a Roe and J. Feigon, *Proc. Natl. Acad. Sci.*, 1993, **90**, 3745–3749.

20 A. Marchand, A. Granzhan, K. Iida, Y. Tsushima, Y. Ma, K. Nagasawa, M.-P. Teulade-Fichou and V. Gabelica, *J. Am. Chem. Soc.*, 2015, **137**, 750–6.

21 M. J. Cavaluzzi and P. N. Borer, *Nucleic Acids Res.*, 2004, **32**, e13.

22 E. Largy, F. Hamon, F. Rosu, V. Gabelica, E. De Pauw, A. Guédin, J.-L. Mergny and M.-P. Teulade-Fichou, *Chemistry*, 2011, **17**, 13274–83.

23 H. Bertrand, D. Monchaud, A. De Cian, R. Guillot, J.-L. Mergny and M.-P. Teulade-Fichou, *Org. Biomol. Chem.*, 2007, **5**, 2555.